Topological sensitivity analysis in heterogeneous anisotropic elasticity problem. Theoretical and computational aspects

S.M. Giusti [a,*], A. Ferrer [b,c], J. Oliver [b,d]

[a] *National Technological University, Regional Faculty of Córdoba (UTN/FRC - CONICET), Maestro M. López esq. Cruz Roja Argentina, X5016ZAA - Córdoba, Argentina*

[b] *CIMNE – Centre Internacional de Metodes Numerics en Enginyeria, Campus Nord UPC, Edifici C-1, c/Jordi Girona 1-3, 08034 Barcelona, Spain*

[c] *Escola Superior d'Enginyeries Industrial, Aeroespacial i Audiovisual de Terrassa, Campus de Terrassa, Edificio TR45. C. Colom, 11 08222 Terrassa, Spain*

[d] *E.T.S. d'Enginyers de Camins, Canals i Ports, Technical University of Catalonia, Campus Nord UPC, Edifici C-1, c/Jordi Girona 1-3, 08034 Barcelona, Spain*

Highlights

- Topological derivative of elastic anisotropic and heterogeneous 2D problem.
- Novel, extremely simple closed formula for the topological sensitivity.
- Full mathematical justifications for the obtained formulas.
- Potential applications to structural topology design.

Abstract

The topological sensitivity analysis for the heterogeneous and anisotropic elasticity problem in two-dimensions is performed in this work. The main result of the paper is an analytical closed-form of the topological derivative for the total potential energy of the problem. This derivative displays the sensitivity of the cost functional (the energy in this case) when a small singular perturbation is introduced in an arbitrary point of the domain. In this case, we consider a small disc with a completely different elastic material. Full mathematical justification for the derived formula, and derivations of precise estimates for the remainders of the topological asymptotic expansion are provided. Finally, the influence of the heterogeneity and anisotropy is shown through some numerical examples of structural topology optimization.

* Corresponding author.

E-mail addresses: sgiusti@frc.utn.edu.ar (S.M. Giusti), aferrer@cimne.upc.edu (A. Ferrer), oliver@cimne.upc.edu (J. Oliver).

1. Introduction

Topological asymptotic analysis allows obtaining an asymptotic expansion of a given shape functional when a geometrical domain is singularly perturbed. This perturbation can be materialized by the insertion of holes, inclusions, source-terms or even cracks. The main concept arising from this analysis is the topological derivative [1]. This derivative measures the sensitivity of the shape functional with respect to the infinitesimal singular domain perturbation and it was rigorously introduced in [2]. Since then, this concept has proven extremely useful in the treatment of a wide range of problems; see, for instance, [3–11]. Concerning the theoretical development of the topological asymptotic analysis, besides the monograph [1], the reader is referred to [12,13].

In order to introduce these concepts, let us consider an open and bounded domain $\Omega \subset \mathbb{R}^2$, see Fig. 1, which is subject to a non-smooth perturbation confined in a small region $\omega_\varepsilon(\widehat{x}) = \widehat{x} + \varepsilon\omega$ of size ε. Here, $\widehat{x}$ is an arbitrary point of Ω and ω is a fixed domain of $\mathbb{R}^2$. Then, we assume that a given shape functional $\mathcal{J}_\varepsilon(\Omega)$, associated to the topologically perturbed domain, admits the following topological asymptotic expansion [1]

$$\mathcal{J}_\varepsilon(\Omega) = \mathcal{J}(\Omega) + f(\varepsilon)\mathcal{T}(\widehat{x}) + o(f(\varepsilon)), \tag{1}$$

where $\mathcal{J}(\Omega)$ is the shape functional associated to the unperturbed domain and $f(\varepsilon)$ is a positive function such that $f(\varepsilon) \to 0$ when $\varepsilon \to 0^+$. The function $\widehat{x} \mapsto \mathcal{T}(\widehat{x})$ is termed the topological derivative of $\mathcal{J}$ at $\widehat{x}$. Therefore, the term $f(\varepsilon)\mathcal{T}(\widehat{x})$ represents a first order correction of $\mathcal{J}(\Omega)$ to approximate $\mathcal{J}_\varepsilon(\Omega)$ in $\widehat{x}$. In this work, the singular perturbation is characterized by a circular disc, denoted B_ε, with boundary ∂B_ε and different constitutive properties, see Fig. 1.

From (1), we obtain the standard definition of the topological derivative by passing to the limit $\varepsilon \to 0^+$:

$$\mathcal{T}(\widehat{x}) = \lim_{\varepsilon \to 0^+} \frac{\mathcal{J}_\varepsilon(\Omega) - \mathcal{J}(\Omega)}{f(\varepsilon)}. \tag{2}$$

Notice that, since we are dealing with singular domain perturbations, the shape functionals $\mathcal{J}_\varepsilon(\Omega)$ and $\mathcal{J}(\Omega)$ are associated to topologically different domains. Therefore, the above limit is not trivial to be calculated. In particular, we need to perform an asymptotic analysis of the shape functional $\mathcal{J}_\varepsilon(\Omega)$ with respect to the small parameter ε, i.e. we need information of $\mathcal{J}_\varepsilon(\Omega)$ when $\varepsilon \to 0^+$. As it will be shown later, the shape functional difference (2) depends on the polarization tensor, which is considered a fundamental concept on the topological derivative topic. This tensor, also known in the literature as *Pólya–Szegö polarization tensor*, arises from the asymptotic analysis in singularly perturbed geometrical domains [14]. This mathematical concept permits to write an asymptotic expansion of the shape functional $\mathcal{J}_\varepsilon(\Omega)$ by means of functions evaluated in the unperturbed domain Ω (without considering B_ε). The polarization tensor is characterized by a matrix – *polarization matrix* – depending only on the constitutive properties of the problem and the shape of the singular domain perturbation [15].

The topological derivative, in its closed form, has been fully developed for a wide range of physical phenomena. Most of them, by considering homogeneous and isotropic constitutive behaviors. In fact, only a few works dealing with heterogeneous and anisotropic material behavior can be found in the literature, and, in general, the derived formulas are given in an abstract form (see, for instance, [12]). Closed and analytical forms for this kind of constitutive behavior have been only developed for heat diffusion problems (see [16–18,2]). For anisotropic elasticity, the existence and properties of the polarization tensor was studied in [19,20]. However, the polarization tensor is given again in an abstract form. A technique for the numerical evaluation of the polarization tensor is presented in [21].

In this work, we derive the topological derivative in its closed form for the total potential energy associated to an anisotropic and heterogeneous elasticity problem. We assume as singular perturbation a small circular inclusion introduced at an arbitrary point of the domain. The constitutive properties of the small disc are also anisotropic and completely different from the elasticity properties of the matrix. In addition, we provide a full mathematical justification of the derived formula, and develop precise estimates for the remainders of the topological asymptotic expansion.

Bearing this in mind, the heterogeneous anisotropic topological derivative concept, can be applied in advanced technological research areas such as topology and structural optimization simultaneously combined with topological material-design. In fact, in multi-scale modeling, for a given microstructure the homogenized constitutive response is, in general, anisotropic. In addition, since in each macroscopical structural point we have a different microstructure, the constitutive homogenized response at the macro-scale varies from point to point, i.e., it is heterogeneous. Therefore,
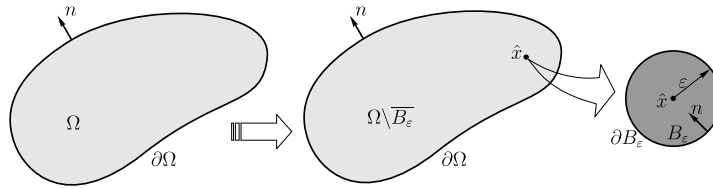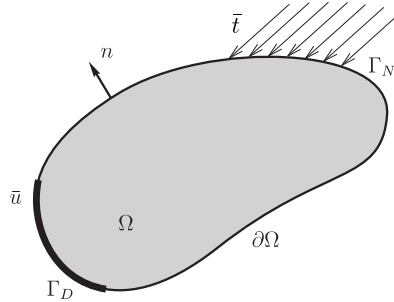
Fig. 1. Topological derivative concept.

Fig. 2. Description of the problem.

for a correct evaluation of the topological sensitivity in a structural optimization problem, a derivative (the topological derivative) for an anisotropic and heterogeneous constitutive behavior is needed.

This paper is organized as follows. Section 2 describes the model associated to an anisotropic and heterogeneous elasticity problem. In Section 3, we present the main result of the paper: a closed formula for the topological derivative. In Section 5, the influence of heterogeneity and anisotropy is shown through some numerical examples for structural topology optimization. The paper is closed in Section 6 where some concluding remarks are presented.

2. Problem formulation

The topological asymptotic analysis of the total potential energy associated to an anisotropic and heterogeneous elasticity problem is calculated. Thus, the unperturbed shape functional is defined as:

$$\mathcal{J}(\Omega) = \frac{1}{2} \int_{\Omega} \sigma(u) \cdot \nabla^s u + \int_{\Gamma_N} \bar{t} \cdot u, \tag{3}$$

where the Cauchy stress tensor $\sigma(u)$ is defined as usual:

$$\sigma(\xi) := \mathbb{C}\nabla^s \xi. \tag{4}$$

In the above equations, $\mathbb{C} = \mathbb{C}(x)$ is a symmetric fourth order elasticity tensor, ∇^s is used to denote the symmetric part of the gradient operator ∇ and u is the displacement field, solution of the following variational problem: find the field $u \in \mathcal{U}$, such that

$$\int_{\Omega} \sigma(u) \cdot \nabla^s \eta + \int_{\Gamma_N} \bar{t} \cdot \eta = 0 \qquad \forall \eta \in \mathcal{V}. \tag{5}$$

In the variational problem (5) the set $\mathcal{U}$ of admissible functions and the space $\mathcal{V}$ of admissible variations are given by

$$\mathcal{U} := \left\{ \phi \in H^1(\Omega; \mathbb{R}^2) : \phi|_{\Gamma_D} = \bar{u} \right\} \quad \text{and} \quad \mathcal{V} := \left\{ \phi \in H^1(\Omega; \mathbb{R}^2) : \phi|_{\Gamma_D} = 0 \right\}. \tag{6}$$

In addition, $\partial\Omega = \overline{\Gamma_N \cup \Gamma_D}$ with $\Gamma_N \cap \Gamma_D = \varnothing$, where Γ_N and Γ_D are Neumann and Dirichlet boundaries, respectively. Thus, $\bar{u}$ is a Dirichlet data on Γ_D and $\bar{t}$ is a Neumann data on Γ_N, both assumed to be smooth enough, see Fig. 2.

On the other hand, for our specific case, we consider a perturbation on the domain given by the nucleation of a small circular inclusion with constitutive properties given by a constant elastic tensor $\mathbb{C}^{\star}$. Therefore, the perturbed shape functional can be written as:

$$\mathcal{J}_{\varepsilon}(\Omega) = \frac{1}{2} \int_{\Omega} \sigma_{\varepsilon}(u_{\varepsilon}) \cdot \nabla^s u_{\varepsilon} + \int_{\Gamma_N} \bar{t} \cdot u_{\varepsilon}, \tag{7}$$

where the stress tensor associated to the perturbed configuration is defined as:

$$\sigma_{\varepsilon}(\xi) := \mathbb{C}_{\varepsilon} \nabla^s \xi. \tag{8}$$

Here, we consider that the inclusion is made of a completely different material. Then, the elasticity tensor $\mathbb{C}_{\varepsilon}$ can be written as follows

$$\mathbb{C}_{\varepsilon} := \begin{cases} \mathbb{C} & \text{in} \quad \Omega \setminus \overline{B_{\varepsilon}} \\ \mathbb{C}^{\star} & \text{in} \quad B_{\varepsilon}. \end{cases} \tag{9}$$

In addition, in (7) the function u_{ε} is solution of the following variational problem:

Find the field $u_{\varepsilon} \in \mathcal{U}_{\varepsilon}$, such that

$$\int_{\Omega} \sigma_{\varepsilon}(u_{\varepsilon}) \cdot \nabla^s \eta + \int_{\Gamma_N} \bar{t} \cdot \eta = 0 \qquad \forall \eta \in \mathcal{V}_{\varepsilon}, \tag{10}$$

and both the set $\mathcal{U}_{\varepsilon}$ and the space $\mathcal{V}_{\varepsilon}$ are defined as

$$\mathcal{U}_{\varepsilon} := \{\phi \in \mathcal{U} : [\![\phi]\!] = 0 \text{ on } \partial B_{\varepsilon}\} \quad \text{and} \quad \mathcal{V}_{\varepsilon} := \{\phi \in \mathcal{V} : [\![\phi]\!] = 0 \text{ on } \partial B_{\varepsilon}\}, \tag{11}$$

where we use $[\![(\cdot)]\!]$ to denote the *jump* of function $(\cdot)$ across the boundary ∂B_{ε}. Note that the domain Ω is topologically perturbed by the introduction of an inclusion $B_{\varepsilon}(\widehat{x})$ with complete different elastic constitutive properties (in general anisotropic).

3. Topological derivative

In this section we present the main result of the work: an analytical formula for the topological derivative of the energy shape functional associated to an anisotropic and heterogeneous elastic problem. We begin by choosing as admissible test function in problems (5) and (10), the function $\eta = u_{\varepsilon} - u$. Then, we obtain as consequence the following expressions

$$\int_{\Omega} \sigma(u) \cdot \nabla^s u = \int_{\Omega} \sigma(u_{\varepsilon}) \cdot \nabla^s u + \int_{\Gamma_N} \bar{t}(u_{\varepsilon} - u), \tag{12}$$

$$\int_{\Omega} \sigma_{\varepsilon}(u_{\varepsilon}) \cdot \nabla^s u_{\varepsilon} = \int_{\Omega} \sigma_{\varepsilon}(u_{\varepsilon}) \cdot \nabla^s u - \int_{\Gamma_N} \bar{t}(u_{\varepsilon} - u). \tag{13}$$

Therefore, the shape functionals (3) and (7) can be written as

$$\mathcal{J}(\Omega) = \frac{1}{2} \int_{\Omega} \sigma(u_{\varepsilon}) \cdot \nabla^s u + \frac{1}{2} \int_{\Gamma_N} \bar{t}(u_{\varepsilon} + u), \tag{14}$$

$$\mathcal{J}_{\varepsilon}(\Omega) = \frac{1}{2} \int_{\Omega} \sigma_{\varepsilon}(u_{\varepsilon}) \cdot \nabla^s u + \frac{1}{2} \int_{\Gamma_N} \bar{t}(u_{\varepsilon} + u). \tag{15}$$

By considering the above results, the difference of the shape functionals $\mathcal{J}_{\varepsilon}(\Omega)$ and $\mathcal{J}(\Omega)$ reads

$$\mathcal{J}_{\varepsilon}(\Omega) - \mathcal{J}(\Omega) = \frac{1}{2} \int_{\Omega} \sigma_{\varepsilon}(u_{\varepsilon}) \cdot \nabla^s u - \frac{1}{2} \int_{\Omega} \sigma(u_{\varepsilon}) \cdot \nabla^s u. \tag{16}$$

Taking into account the definitions of the perturbed elasticity tensor $\mathbb{C}_\varepsilon$ and perturbed stress tensor, we have that the difference of the total potential energy is given by an integral concentrated in the inclusion B_ε, namely

$$\mathcal{J}_\varepsilon(\Omega) - \mathcal{J}(\Omega) = \frac{1}{2} \int_{B_\varepsilon} \Delta\mathbb{C}(\mathbb{C}^\star)^{-1} \sigma_\varepsilon(u_\varepsilon) \cdot \nabla^s u, \tag{17}$$

with $\Delta\mathbb{C} := \mathbb{C}^\star - \mathbb{C}$.

Let us assume that the elasticity tensor $\mathbb{C}(x)$ is smooth enough such that it admits an expansion in Taylor series around the point $\widehat{x}$ of the form $\mathbb{C}(x) = \mathbb{C}(\widehat{x}) + \nabla\mathbb{C}(\zeta)(x - \widehat{x})$, where $\zeta \in (x, \widehat{x})$. Now, in order to analytically solve the integral (17), we introduce the following ansatz proposed in [22] for the solution associated to the perturbed problem u_ε:

$$u_\varepsilon(x) = u(x) + \varepsilon w(x/\varepsilon) + \widetilde{u}_\varepsilon(x), \tag{18}$$

where the function $w(y)$ is the solution of the following exterior problem independent of the small parameter ε

$$\begin{cases} \text{div}\,(\sigma_\varepsilon(w)) = 0 & \text{in } \mathbb{R}^2 \\ \sigma_\varepsilon(w) = \mathbb{C}_\varepsilon(\widehat{x})\nabla^s w & \\ w \to 0 & \text{at } \infty \\ [\![w]\!] = 0 & \text{on } \partial B_1 \\ [\![\sigma_\varepsilon(w)]\!]n = -\mathbb{S}\sigma(u)(\widehat{x})n & \text{on } \partial B_1, \end{cases} \tag{19}$$

where $\mathbb{S} := \mathbb{I} - \mathbb{C}^\star\mathbb{C}^{-1}$, $\mathbb{I}$ denote the fourth-order identity tensor and was used the change of variable $x = \varepsilon y$. The remainder $\widetilde{u}_\varepsilon$ in (18) must satisfy the following equation:

$$\begin{cases} \text{div}(\sigma_\varepsilon(\widetilde{u}_\varepsilon)) = \varepsilon\text{div}(\nabla\mathbb{C}_\varepsilon(\zeta)(x - \widehat{x})\nabla^s w) & \text{in } \Omega \\ \widetilde{u}_\varepsilon = -\varepsilon w & \text{on } \Gamma_D \\ \sigma(\widetilde{u}_\varepsilon)n = -\varepsilon\sigma(w)n & \text{on } \Gamma_N \\ [\![\widetilde{u}_\varepsilon]\!] = 0 & \text{on } \partial B_\varepsilon \\ [\![\sigma_\varepsilon(\widetilde{u}_\varepsilon)]\!]n = -\varepsilon[\![(\nabla\mathbb{C}_\varepsilon(\zeta)\,n)\,(\nabla^s u(\widehat{x}) + \nabla^s w)]\!]n & \text{on } \partial B_\varepsilon, \end{cases} \tag{20}$$

which has the following estimate $\|\widetilde{u}_\varepsilon\|_{H^1(\Omega;\mathbb{R}^2)} \leq C\varepsilon$, with the constant C independent of ε (see Appendix A). The exterior problem (19) is solved explicitly in Appendix B by using the complex variable method [23,24]. From (B.17), the stress tensor $\sigma_\varepsilon(w)$ inside the inclusion B_ε can be written as:

$$\sigma_\varepsilon(w)|_{B_\varepsilon(\widehat{x})} = \mathbb{T}\sigma(u)(\widehat{x}), \tag{21}$$

where $\mathbb{T} := -\mathbb{A}\mathbb{S}$ and the fourth order tensor $\mathbb{A}$ is shown in (B.18) of Appendix B.

Taking into account (18), the difference of shape functionals (17) reads

$$\mathcal{J}_\varepsilon(\Omega) - \mathcal{J}(\Omega) = \frac{1}{2} \int_{B_\varepsilon} \Delta\mathbb{C}(\mathbb{C}^\star)^{-1}(\sigma_\varepsilon(u) + \sigma_\varepsilon(w)) \cdot \nabla^s u + \mathcal{E}(\varepsilon), \tag{22}$$

where the term $\mathcal{E}(\varepsilon)$ is given by

$$\mathcal{E}(\varepsilon) = \frac{1}{2} \int_{B_\varepsilon} \Delta\mathbb{C}(\mathbb{C}^\star)^{-1} \sigma_\varepsilon(\widetilde{u}_\varepsilon) \cdot \nabla^s u, \tag{23}$$

which has the following estimate $\mathcal{E}(\varepsilon) = o(\varepsilon^2)$ as shown in Appendix A. Next, by using the interior elliptic regularity of the function u in B_ε, the difference of the shape functionals (22) satisfies the following identity:

$$\mathcal{J}_\varepsilon(\Omega) - \mathcal{J}(\Omega) = \frac{1}{2} \int_{B_\varepsilon} \Delta\mathbb{C}(\widehat{x})(\mathbb{C}^\star)^{-1}(\sigma_\varepsilon(u)(\widehat{x}) + \sigma_\varepsilon(w)) \cdot \nabla^s u(\widehat{x}) + o(\varepsilon^2), \tag{24}$$

where the expansion of the tensor $\mathbb{C}(x)$ has been used again.

With the use of (21) and the change of variables $x = \varepsilon y$ the above expression can be analytically solved leading to

$$\mathcal{J}_\varepsilon(\Omega) - \mathcal{J}(\Omega) = \pi\varepsilon^2\mathbb{P}\sigma(u)(\widehat{x}) \cdot \nabla^s u(\widehat{x}) + o(\varepsilon^2), \tag{25}$$

where $\mathbb{P}$ can be recognized as the Pólya–Szegö polarization tensor, given explicitly by

$$\mathbb{P} = \frac{1}{2} \Delta \mathbb{C}(\widehat{x})[(\mathbb{C}(\widehat{x}))^{-1} + (\mathbb{C}^{\star})^{-1}\mathbb{T}]. \tag{26}$$

Finally, using the definition (1) and taking $f(\varepsilon) = |B_{\varepsilon}| = \pi \varepsilon^2$, the topological derivative for the problem under consideration is given explicitly by

$$\mathcal{T}(\widehat{x}) = \mathbb{P}\sigma(u)(\widehat{x}) \cdot \nabla^s u(\widehat{x}) \qquad \forall \widehat{x} \in \Omega. \tag{27}$$

Note that this formula is general, in the sense that measures the sensitivity of the total potential energy when two materials with completely different constitutive tensors are considered. Also, the polarization tensor $\mathbb{P}$ depends only on the constitutive tensors $\mathbb{C}(\widehat{x})$ and $\mathbb{C}^{\star}$. This means that once defined $\mathbb{C}$ and $\mathbb{C}^{\star}$ for the point $\widehat{x}$, the tensor $\mathbb{P}$ can be easily obtained by computing the components of $\mathbb{A}$, see Appendix B, and consequently so is $\mathbb{T}$.

Remark 1. From the final expression for the polarization tensor associated to the anisotropic and heterogeneous elasticity problem (26), we can analyze the limit case when the inclusion becomes a hole by taking the limit when $\mathbb{C}^{\star} \to 0$. On the other hand, to analyze the sensitivity to the introduction of a rigid inclusion, we need to take the limit when $\mathbb{C}^{\star} \to \infty$. It should be noted that both limits exist and they can be easily obtained.

Remark 2. If we consider that both materials are isotropic, with constitutive properties E and ν (background material), and $E^{\star}$ and $\nu^{\star}$ (inclusion), the polarization tensor (26) can be written for plane stress as a fourth-order isotropic polarization tensor, as:

$$\mathbb{P} = -\frac{1}{2} \frac{1}{\beta\gamma + \tau_1} \left[(1+\beta)(\tau_1 - \gamma)\mathbb{I} + \frac{1}{2}(\alpha - \beta) \frac{\gamma(\gamma - 2\tau_3) + \tau_1\tau_2}{\alpha\gamma + \tau_2}(I \otimes I) \right], \tag{28}$$

where

$$\alpha = \frac{1+\nu}{1-\nu}, \ \beta = \frac{3-\nu}{1+\nu}, \ \gamma = \frac{E^{\star}}{E}, \ \tau_1 = \frac{1+\nu^{\star}}{1+\nu}, \ \tau_2 = \frac{1-\nu^{\star}}{1-\nu} \quad \text{and} \quad \tau_3 = \frac{\nu^{\star}(3\nu - 4) + 1}{\nu(3\nu - 4) + 1}. \tag{29}$$

Note that by considering $\nu^{\star} = \nu$, the parameters $\tau_i = 1$ (with $i = 1..3$) and (28) becomes the polarization tensor for isotropy elasticity widely used in structural topological design [1].

4. Numerical validation

The analytical formula for the topological derivative presented in (27), can be validated by using the computational framework described in this section. To this end, we define (for a finite value of ε) the function $T_{\varepsilon}(\widehat{x})$ as:

$$T_{\varepsilon}(\widehat{x}) := \frac{\mathcal{J}_{\varepsilon}(\Omega) - \mathcal{J}(\Omega)}{f(\varepsilon)}. \tag{30}$$

Clearly, the above definition has the following property,

$$\lim_{\varepsilon \to 0} T_{\varepsilon}(\widehat{x}) = \mathcal{T}(\widehat{x}). \tag{31}$$

A numerical approximation of $\mathcal{T}(\widehat{x})$ can be obtained by calculating the functions $\mathcal{J}_{\varepsilon}(\Omega)$ and $\mathcal{J}(\Omega)$, for a sequence of decreasing values of ε and then using (30) to compute the corresponding estimates $T_{\varepsilon}(\widehat{x})$ for $\mathcal{T}(\widehat{x})$. The values of the function $\mathcal{J}$ and $\mathcal{J}_{\varepsilon}$ are computed numerically by means of standard finite element procedure for the elasticity problem. The domain considered in the verification is a unit square. The perturbed domains are obtained by introducing circular inclusions of radii

$$\varepsilon \in \{0.160, 0.080, 0.040, 0.010, 0.005\}, \tag{32}$$

centered at $\widehat{x} = (0.5, 0.5)$, with the origin of the coordinate system positioned at the bottom left corner. The finite element mesh used to discretize the perturbed domain contains a total number of 3 850 240 three-nodded elements and 1 926 401 nodes.
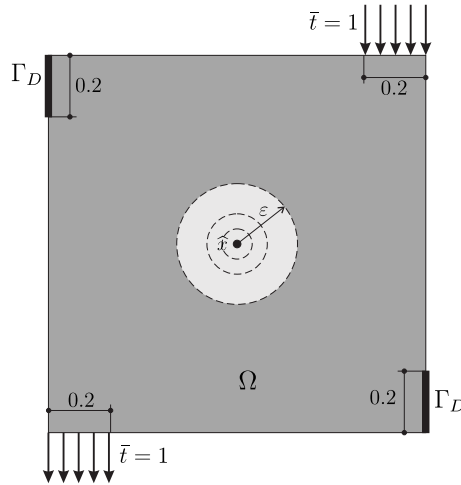
Fig. 3. Domain and boundary conditions.

To solve the anisotropic elastic problem, we prescribe the displacement on Γ_D to be $\bar{u} = 0$ and traction $\bar{t} = 1$ on Γ_N, see Fig. 3.

The study is conducted for four combinations of elasticity tensors $\mathbb{C}$ and $\mathbb{C}^\star$. The analyzed cases are given by:

$$
\begin{array}{lll}
\text{Case 1} & \mathbb{C} = \begin{pmatrix} 0.905 & 0.845 & -0.017 \\ 0.845 & 1.405 & -0.415 \\ -0.017 & -0.415 & 0.385 \end{pmatrix} & \mathbb{C}^\star = \begin{pmatrix} 1.562 & 0.312 & 0.0 \\ 0.312 & 1.562 & 0.0 \\ 0.0 & 0.0 & 0.625 \end{pmatrix} \\[4ex]
\text{Case 2} & \mathbb{C} = \begin{pmatrix} 1.099 & 0.329 & 0.0 \\ 0.329 & 1.099 & 0.0 \\ 0.0 & 0.0 & 0.385 \end{pmatrix} & \mathbb{C}^\star = \begin{pmatrix} 1.562 & 0.312 & 0.0 \\ 0.312 & 1.562 & 0.0 \\ 0.0 & 0.0 & 0.625 \end{pmatrix} \\[4ex]
\text{Case 3} & \mathbb{C} = \begin{pmatrix} 2.083 & 0.416 & 0.0 \\ 0.416 & 4.160 & 0.0 \\ 0.0 & 0.0 & 0.833 \end{pmatrix} & \mathbb{C}^\star = \begin{pmatrix} 1.099 & 0.329 & 0.0 \\ 0.329 & 1.099 & 0.0 \\ 0.0 & 0.0 & 0.385 \end{pmatrix} \\[4ex]
\text{Case 4} & \mathbb{C} = \begin{pmatrix} 2.083 & 0.416 & 0.0 \\ 0.416 & 4.160 & 0.0 \\ 0.0 & 0.0 & 0.833 \end{pmatrix} & \mathbb{C}^\star = \begin{pmatrix} 0.905 & 0.845 & -0.017 \\ 0.845 & 1.405 & -0.415 \\ -0.017 & -0.415 & 0.385 \end{pmatrix}
\end{array}
$$

The normalized obtained results $(T_\varepsilon/\mathcal{T})$ are plotted in Fig. 4, where the analytical topological derivative and the numerical approximations for each value of ε are shown. It can be seen that the numerical topological derivatives converge to the corresponding analytical value for all cases. This confirms the validity of the proposed formula (27).

5. Numerical examples

In order to evidence the potential application of the topological derivative concept for anisotropic and heterogeneous materials, some numerical examples are shown in this section.

5.1. Numerical algorithm

As usual in the topological optimization scientific community, a minimum compliance objective function, subject to a certain fraction volume, will be solved. To this end, the material distribution in Ω will be identified by a characteristic function χ. Thus, the objective function $\mathcal{J}(\Omega)$ can be written as a function of χ as: $\mathcal{J}(\Omega_\chi)$, where Ω_χ is used to denote the geometrical dependency of the domain on the characteristic function χ. Then, the optimization problem is:
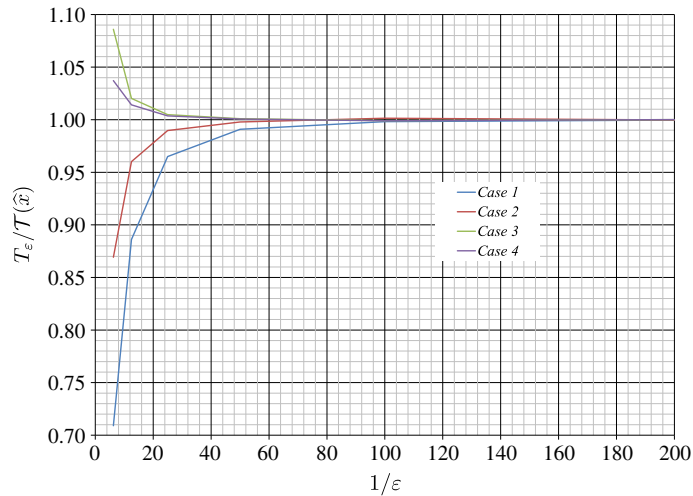
Fig. 4. Results of numerical verification.

Find the characteristic function χ such that,

$$
\begin{aligned}
&\min_{\chi} && \mathcal{J}(\Omega_\chi) \\
&\text{s.t.} && c(\chi) = \int_\Omega \chi - V = 0,
\end{aligned}
\tag{33}
$$

where $\mathcal{J}(\Omega_\chi)$ is the total potential energy of a standard elastic equilibrium problem (5) and V the final intended volume. Note that the constitutive tensor $\mathbb{C}$ could be heterogeneous and anisotropic.

An efficient approach to solve problem (33) is the use of the method proposed in [25]. The procedure relies on a level-set domain representation [26] and the approximation of the topological optimality conditions by a fixed point iteration. The topological derivative (27) is used as a feasible descent direction to minimize the cost function $\mathcal{J}(\Omega_\chi)$. This class of algorithm has been successfully used in research areas related to topological optimization such as: microstructure of materials [27], load bearing structures subjected to point-wise stress constraint [28,6] and piezoelectric actuators [3]. For completeness, in the following, some remarks about the algorithm are detailed. For further details we refer to the work by [6,25].

- The definition of the domain lies on the level set function ψ. The design variable is no longer the characteristic function χ. In fact, it is parametrized by the level set ψ as

$$
\chi(x) = \begin{cases} 1 & \psi(x) < 0, \\ 0 & \psi(x) > 0. \end{cases}
\tag{34}
$$

- In order to satisfy the constraint $c(\chi) = 0$, as in [29,30], an augmented Lagrangian method is used. Thereby, a Lagrange multiplier λ appears as a new unknown, and a penalty parameter ρ must be provided. The optimization problem (33) becomes the following saddle point problem,

$$
\max_{\lambda} \min_{\psi} \quad \mathcal{J}(\Omega_\psi) + \lambda c(\psi) + \frac{1}{2}\rho c(\psi)^2.
\tag{35}
$$

- An extended topological derivative is defined as,

$$
g(x) = \begin{cases} -\mathcal{T}(x) - \max(0, \lambda + \rho c(\psi)) & \psi(x) < 0, \\ \mathcal{T}(x) + \max(0, \lambda + \rho c(\psi)) & \psi(x) > 0. \end{cases}
\tag{36}
$$

Fig. 5. Schematic drawing of a traction rod with homogeneous material distribution.

- The optimality condition, see [31], is based on seeking $\psi(x)$ parallel to $g(x)$ and unitary. Thus, a slerp interpolation scheme is used, i.e.,

$$\psi_{n+1} = \frac{1}{\sin\theta_n}\left[\sin((1-\kappa_n)\theta_n)\psi_n + \sin(\kappa_n\theta_n)\frac{g_n}{\|g_n\|_{L^2}}\right], \tag{37}$$

where $\kappa_n \in [0, 1]$ is a line search-like parameter and the converge criterion is based on the value of θ_n, the angle between ψ_n and g_n, which is written as

$$\theta_n = \mathrm{acos}\left[\frac{\langle\psi_n, g_n\rangle}{\|\psi\|_{L^2}\|g_n\|_{L^2}}\right]. \tag{38}$$

Note that, in this fix point scheme, the topological derivative for anisotropic materials plays the role of the gradient in a steepest descent algorithm. With this algorithm, some numerical examples, both with homogeneous and heterogeneous material distribution, are considered. All of them are solved under 2D elastic plane stress assumptions. Regarding to numerical aspects, a standard FEM is used for solving (5).

5.2. Representative numerical simulations

In this first set of case studies, the constitutive behavior is homogeneous in the design domain. Besides, the constitutive tensor in the inclusion is defined with the contrast parameter γ as follows: $\mathbb{C}^\star = \gamma\mathbb{C}$ with $\gamma = 10^{-4}$. The 2×1 domain is discretized with a structured mesh of 5200 P1 triangular elements. The volume fraction is taken as $V = 0.4$ and the penalty as $\rho = 0.5$. All the examples are declared to be converged when $\theta < 1°$ and $|c(\psi)| < 0.001$. In the figures showing the obtained results, the black and white colors are used to represent the part of the domain with constitutive tensor $\mathbb{C}$ and $\mathbb{C}^\star$, respectively. Note that, the elasticity of the inclusion is weak enough to mimic a void.

5.2.1. Homogeneous material distribution—Traction rod

As shown in Fig. 5, regarding to boundary conditions, the domain is fixed at the left side and has a horizontal unitary force at the middle of the right end. Some representative cases, in terms of the definition of the constitutive tensor, have been selected (see second column in Fig. 6).

In the second column, the constitutive tensor used is shown, which is obtained by a classical homogenization procedure of the micro-structure displayed on the third column, see [32]. In the fourth one, the final optimal topology for the structure is also shown.

Notice the strong influence of the selected micro-structure topology and, consequently, of the resulting homogenized constitutive tensor, on the obtained optimal macro-structure topology.

5.2.2. Homogeneous material distribution—Cantilever beam

Now a standard cantilever beam is solved. All data are as before, except for the direction of the applied force (see Fig. 7).

The isotropic case is used also as a reference. Some unconventional topologies are obtained, specially in the orthotropic case (micro-structure with horizontal and vertical bars) and full anisotropic case (last row). It can be observed, that the resulting macro-structure topology, tends to arrange following the principal directions of the micro-structure topology.

Case	Constitutive tensor	Micro-structure	Optimal topology	Compliance
a)	$\mathbb{C} = \begin{pmatrix} 1.0989 & 0.3297 & 0 \\ 0.3297 & 1.0989 & 0 \\ 0 & 0 & 0.3846 \end{pmatrix}$			6.525
b)	$\mathbb{C} = \begin{pmatrix} 0.5697 & 0.0231 & 0 \\ 0.0231 & 0.0784 & 0 \\ 0 & 0 & 0.0070 \end{pmatrix}$			23.654
c)	$\mathbb{C} = \begin{pmatrix} 0.0784 & 0.0231 & 0 \\ 0.0231 & 0.5697 & 0 \\ 0 & 0 & 0.0070 \end{pmatrix}$			101.304
d)	$\mathbb{C} = \begin{pmatrix} 0.2867 & 0.1900 & 0 \\ 0.1900 & 0.2867 & 0 \\ 0 & 0 & 0.1715 \end{pmatrix}$			24.949
e)	$\mathbb{C} = \begin{pmatrix} 0.3400 & 0.1689 & 0 \\ 0.1689 & 0.3400 & 0 \\ 0 & 0 & 0.1401 \end{pmatrix}$			24.298
f)	$\mathbb{C} = \begin{pmatrix} 0.2479 & 0.1208 & 0.1178 \\ 0.1208 & 0.2050 & 0.0613 \\ 0.1178 & 0.0613 & 0.1391 \end{pmatrix}$			23.512

Fig. 6. Representative optimal homogeneous traction rod topologies: (a) Isotropic ($E = 1$ and $\nu = 0.3$) as a reference, (b)–(e) Orthotropic, (f) Anisotropic.

Fig. 7. Schematic drawing of a cantilever beam with homogeneous material distribution.

5.2.3. Heterogeneous material distribution

In the following set of examples, a heterogeneous distribution of material is used for a classical cantilever beam optimal design. The contrast parameter is taken $\gamma = 10^{-4}$. The 2×1 domain is discretized through a structured mesh of 6272 P1 elements. The geometry is vertically partitioned in four domains with the same width (1/4). The top and bottom regions are endowed with a constitutive tensor different from the center one (see Figs. 9 and 11). The intended volume fraction is $V = 0.4$ and the considered penalty value is $\rho = 0.5$. Again the iterative solution algorithm is declared converged when $\theta < 1°$ and $|c(\psi)| < 0.001$.

– *Case* 1. In this example, the top and bottom regions are endowed with a microstructure topology yielding horizontally-dominant microscopic stiffness, where the center region, microscopic topology enforces shear-dominant stiffness.

The material arrangement and distribution are sketched in Fig. 9. The corresponding values for the resulting homogenized constitutive properties are detailed in Fig. 10.

It is worth noting that both constitutive tensors are again anisotropic. In addition, note that the optimal topology with the anisotropic heterogeneous material distribution is quite different from the homogeneous isotropic case (first row of Fig. 8) and the homogeneous anisotropic case (last row of Fig. 8). Again, it can be observed as the macroscopic topology tends to mimic the microscopic one in the different considered regions.

Case	Constitutive tensor	Micro-structure	Optimal topology	Compliance
a)	$\mathbb{C} = \begin{pmatrix} 1.0989 & 0.3297 & 0 \\ 0.3297 & 1.0989 & 0 \\ 0 & 0 & 0.3846 \end{pmatrix}$			71.392
b)	$\mathbb{C} = \begin{pmatrix} 0.5697 & 0.0231 & 0 \\ 0.0231 & 0.0784 & 0 \\ 0 & 0 & 0.0070 \end{pmatrix}$			892.328
c)	$\mathbb{C} = \begin{pmatrix} 0.0784 & 0.0231 & 0 \\ 0.0231 & 0.5697 & 0 \\ 0 & 0 & 0.0070 \end{pmatrix}$			1685.169
d)	$\mathbb{C} = \begin{pmatrix} 0.2867 & 0.1900 & 0 \\ 0.1900 & 0.2867 & 0 \\ 0 & 0 & 0.1715 \end{pmatrix}$			335.980
e)	$\mathbb{C} = \begin{pmatrix} 0.3400 & 0.1689 & 0 \\ 0.1689 & 0.3400 & 0 \\ 0 & 0 & 0.1401 \end{pmatrix}$			251.031
f)	$\mathbb{C} = \begin{pmatrix} 0.2782 & 0.1250 & 0.0728 \\ 0.1250 & 0.2184 & 0.0120 \\ 0.0728 & 0.0120 & 0.1416 \end{pmatrix}$			224.387

Fig. 8. Representative optimal homogeneous traction rod topologies: (a) Isotropic ($E = 1$ and $\nu = 0.3$) as a reference, (b)–(e) Orthotropic, (f) Anisotropic.
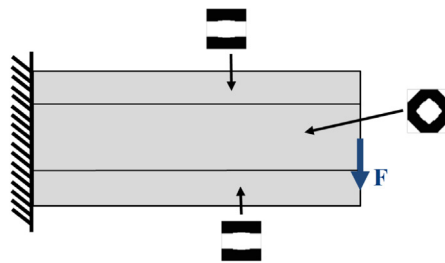

Fig. 9. Heterogeneous cantilever beam with regions of different constitutive properties (enforced via microscopic material topology).

Constitutive tensor	Micro-structure	Optimal topology	Compliance
$\mathbb{C} = \begin{pmatrix} 0.5697 & 0.0231 & 0 \\ 0.0231 & 0.0784 & 0 \\ 0 & 0 & 0.0070 \end{pmatrix}$			309.095
$\mathbb{C} = \begin{pmatrix} 0.2867 & 0.1900 & 0 \\ 0.1900 & 0.2867 & 0 \\ 0 & 0 & 0.1715 \end{pmatrix}$			

Fig. 10. Heterogeneous cantilever beam. Material properties and obtained results (case 1).

– *Case* 2. Now the top and bottom regions are endowed with a microstructure yielding horizontally-dominant elastic stiffness, whereas the central region is endowed with a vertically-dominant one.

Fig. 11 shows a schematic picture of this case. Details of the resulting homogenized elastic properties are given in Fig. 12.

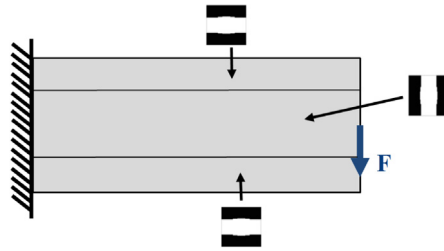In Fig. 12, the resulting (non trivial) optimal topology obtained for this case is shown.

Fig. 11. Heterogeneous cantilever beam. Material properties and obtained results (case 2).

Constitutive tensor		Micro-structure	Optimal topology	Compliance
$\mathbb{C} = \begin{pmatrix} 0.5697 & 0.0231 & 0 \\ 0.0231 & 0.0784 & 0 \\ 0 & 0 & 0.0070 \end{pmatrix}$				996.863
$\mathbb{C} = \begin{pmatrix} 0.0784 & 0.0231 & 0 \\ 0.0231 & 0.5697 & 0 \\ 0 & 0 & 0.0070 \end{pmatrix}$				

Fig. 12. Optimal heterogeneous Cantilever beam topology. Constitutive tensor value and its corresponding micro-structure representation are also detailed.

Regarding numerical aspects, problems of convergence of the involved numerical schemes have not been found.

Besides, no substantial differences, in terms of the involved computational effort, have been found by considering the isotropic and anisotropic cases. In all cases less than five minutes of computation are needed with a standard PC (3.40 GHz processor in a 64-bit architecture) in a Matlab$^{©}$ environment.

6. Concluding remarks

In this work an analytical and closed-form expression for the topological derivative in heterogeneous and anisotropic elastic problems has been presented. We consider as singular perturbation the introduction of a circular disc, with an anisotropic constitutive tensor completely different from the background material, in an arbitrary point. From the asymptotic analysis, it has been proven that the heterogeneous behavior of the material properties does not contribute to the first order topological derivative. The polarization tensor for this problem is obtained from a very simple (and inexpensive) matrix evaluation, in terms of the constitutive properties of the unperturbed problem and the inclusion. The derived formula is general for any kind of anisotropy in two dimensional problems, where orthotropy and isotropy (of the background material or the inclusion or a combination of both) can be derived as particular cases.

We recall that the development presented in this work for the total potential energy, in particular the solution of the so-called exterior problem, can be applied for other cost functionals and that the derivation of the associated topological derivative can be easily done.

With these results in mind, the presented numerical simulation shows that the selected material properties heavily affect the optimal topology in a standard topology optimization problem. Since real applications involve non-homogeneous isotropic material, the obtained closed formula of the topological derivative for heterogeneous anisotropic materials generalizes the concept of topology optimization for any kind of material properties and distribution.

In addition, a certain influence of the microscopic topology on the optimal macroscopic topology is observed which, in some cases, becomes very relevant. This suggests a possible approach, based on the use of the anisotropic topological derivative, to link the microscopic and macroscopic topologies in optimal topological designs. This issue is left for future research.

Acknowledgments

Project "Advanced tools for computational design of engineering materials" COMP-DES-MAT). The work of S.M. Giusti was partially supported by Argentinean Agencies: ANPCyT (National Agency for Scientific and Technical Promotion), PID-UTN (Research and Development Program of the National Technological University) and CONICET (National Council for Scientific and Technical Research), under grants N PICT 2014-3372, PID/UTN 2050-2013 and PIP 2013-631, respectively. The support of all these agencies is gratefully acknowledged.

Appendix A. Estimation of the remainders

In this section the estimation of the remainders in the topological asymptotic expansion is performed. This estimation has been used in the derivation of the topological derivative expression (27) presented in Section 3. In particular, we study the asymptotic behavior of the remainder $\widetilde{u}_\varepsilon$ in (20) and the residue $\mathcal{E}(\varepsilon)$ defined in (23). Let us start by introducing the following lemma that ensures the existence of the topological derivative for the problem under analysis:

Lemma 3. *Let u and u_ε be solutions to (5) and (10), respectively. Then, we have that the estimate $\|u_\varepsilon - u\|_{H^1(\Omega;\mathbb{R}^2)} = O(\varepsilon)$ holds true.*

Proof. We start by subtracting the variational problems (5) and (10) to obtain:

$$\int_\Omega \sigma_\varepsilon(u_\varepsilon - u) \cdot \nabla^s \eta = \int_{B_\varepsilon} \mathbb{S}\sigma(u) \cdot \nabla^s \eta \tag{A.1}$$

with $\mathbb{S} = \mathbb{I} - \mathbb{C}^\star \mathbb{C}^{-1}$. Now, by taking $\eta = u_\varepsilon - u$ as test function in the above equation, we obtain the following equality:

$$\int_\Omega \sigma_\varepsilon(u_\varepsilon - u) \cdot \nabla^s(u_\varepsilon - u) = \int_{B_\varepsilon} \mathbb{S}\sigma(u) \cdot \nabla^s(u_\varepsilon - u). \tag{A.2}$$

From the Cauchy–Schwarz and Poincaré inequality it follows that

$$\int_\Omega \sigma_\varepsilon(u_\varepsilon - u) \cdot \nabla^s(u_\varepsilon - u) \leq C_1 \|\sigma(u)\|_{L^2(B_\varepsilon;\mathbb{R}^2)} \|\nabla^s(u_\varepsilon - u)\|_{L^2(B_\varepsilon;\mathbb{R}^2)}$$
$$\leq C_2\varepsilon \|\nabla^s(u_\varepsilon - u)\|_{L^2(B_\varepsilon;\mathbb{R}^2)}$$
$$\leq C_3\varepsilon \|\nabla^s(u_\varepsilon - u)\|_{H^1(\Omega;\mathbb{R}^2)}$$
$$\leq C_4\varepsilon \|u_\varepsilon - u\|_{H^1(\Omega;\mathbb{R}^2)}, \tag{A.3}$$

where we have used the elliptic regularity of function u. Finally, from the coercivity of the bilinear form of (10), namely

$$c\|u_\varepsilon - u\|_{H^1(\Omega;\mathbb{R}^2)}^2 \leq \int_\Omega \sigma_\varepsilon(u_\varepsilon - u) \cdot \nabla^s(u_\varepsilon - u), \tag{A.4}$$

we obtain the result with the constant C_4/c independent of the small parameter ε.

Lemma 4. *Let $\widetilde{u}_\varepsilon$ be solution to (20). Then, the following estimate holds true:*

$$\|\widetilde{u}_\varepsilon\|_{H^1(\Omega;\mathbb{R}^2)} \leq C\varepsilon, \tag{A.5}$$

with the constant C independent of the small parameter ε.

Proof. From the ansatz proposed in (18) for u_ε and making use of the triangular inequality, we obtain:

$$|\widetilde{u}_\varepsilon|_{H^1(\Omega;\mathbb{R}^2)} = |u_\varepsilon - u - \varepsilon w|_{H^1(\Omega;\mathbb{R}^2)}$$
$$\leq |u_\varepsilon - u|_{H^1(\Omega;\mathbb{R}^2)} + \varepsilon|w|_{H^1(\Omega;\mathbb{R}^2)}$$
$$\leq \|u_\varepsilon - u\|_{H^1(\Omega;\mathbb{R}^2)} + \varepsilon|w|_{H^1(\mathbb{R}^2;\mathbb{R}^2)}$$
$$\leq C_1\varepsilon, \tag{A.6}$$

where we have used the change of variables $x = \varepsilon y$, the equivalence between the semi-norm and the norm in $H^1(\Omega;\mathbb{R}^2)$ and the estimate in Lemma 3. Finally, the results come out from the Poincaré inequality.

Lemma 5. *Let $\widetilde{u}_\varepsilon$ and u be solutions to* (20) *and* (5) *, respectively. Then, we have the following estimate for the remainder $\mathcal{E}(\varepsilon)$ in* (23)*:*

$$\frac{1}{2}\int_{B_\varepsilon} \Delta\mathbb{C}(\mathbb{C}^\star)^{-1}\sigma_\varepsilon(\widetilde{u}_\varepsilon)\cdot\nabla^s u = o(\varepsilon^2). \tag{A.7}$$

Proof. From the Cauchy–Schwarz inequality we obtain

$$\begin{aligned}
\mathcal{E}(\varepsilon) &= \frac{1}{2}\int_{B_\varepsilon} \Delta\mathbb{C}(\mathbb{C}^\star)^{-1}\sigma_\varepsilon(\widetilde{u}_\varepsilon)\cdot\nabla^s u \\
&\le C_1\|\nabla^s u\|_{L^2(B_\varepsilon;\mathbb{R}^2)}\|\nabla^s\widetilde{u}_\varepsilon\|_{L^2(B_\varepsilon;\mathbb{R}^2)} \\
&\le \varepsilon C_2\|\nabla^s\widetilde{u}_\varepsilon\|_{L^2(B_\varepsilon;\mathbb{R}^2)}.
\end{aligned} \tag{A.8}$$

Note that from problem (20) that the r.h.s. depends explicitly on the small parameter ε. Therefore, since this problem is linear and in view of Lemma 4, we can write $\widetilde{u}_\varepsilon = \varepsilon v_0$. Then, we have

$$\begin{aligned}
\mathcal{E}(\varepsilon) &\le \varepsilon^2 C_3\|\nabla^s v_0\|_{L^2(B_\varepsilon;\mathbb{R}^2)} \\
&\le \varepsilon^3 C_4
\end{aligned} \tag{A.9}$$

which leads to the result.

Appendix B. Solution of the exterior problem

In this section we show the analytical solution of the problem presented in (19). In particular, we present the solution of a generalized version of problem (19), namely,

$$\begin{cases}
\text{div}\,(\sigma_\varepsilon(w)) = 0 & \text{in }\ \mathbb{R}^2 \\
\sigma_\varepsilon(w) = \mathbb{C}_\varepsilon(\widehat{x})\nabla^s w & \\
w \to 0 & \text{at }\ \infty \\
[\![w]\!] = 0 & \text{on }\ \partial B_1 \\
[\![\sigma_\varepsilon(w)]\!]n = Sn & \text{on }\ \partial B_1,
\end{cases} \tag{B.1}$$

where S is a symmetric second order tensor.

A general methodology to solve problem (B.1) can be constructed by using the *complex variable method* for anisotropic elasticity [23,24]. Now we briefly present the main steps to solve the above problem. A complete description of the methodology and its application can be found in above cited books.

First we define a new coordinate system $z_i = x + \mu_i y$ for $i = 1..2$, where μ_i are complex parameters, roots of the following equation:

$$\alpha_{11}\mu^4 - 2\alpha_{13}\mu^3 + (2\alpha_{12} + \alpha_{33})\mu^2 - 2\alpha_{23}\mu + \alpha_{22} = 0 \tag{B.2}$$

where α_{ij}, with $(i, j) = 1..3$, are the components of $\mathbb{C}^{-1}$ (in matrix notation). Two cases are possible, depending on the relations between the elastic constant: (i) the roots are all different: μ_1, μ_2, $\bar{\mu}_1$ and $\bar{\mu}_2$; and (ii) the roots are pairwise equal: $\mu_1 = \mu_2$ and $\bar{\mu}_1 = \bar{\mu}_2$. Here, $\bar{\mu}_1$ and $\bar{\mu}_2$ denote the complex conjugates of parameters μ_1 and μ_2. Based on the previous definitions, a general expression for the stress components can be obtained as:

$$\begin{aligned}
(\sigma_\varepsilon(w))_{xx} &= 2\Re[\mu_1^2\Phi_1'(z_1) + \mu_2^2\Phi_2'(z_2)], \\
(\sigma_\varepsilon(w))_{yy} &= 2\Re[\Phi_1'(z_1) + \Phi_2'(z_2)], \\
(\sigma_\varepsilon(w))_{xy} &= -2\Re[\mu_1\Phi_1'(z_1) + \mu_2\Phi_2'(z_2)],
\end{aligned} \tag{B.3}$$

with $\Re[\bullet]$ denoting the real part of $[\bullet]$ and the prime is used to denote the derivative for the function $f(z)$ respect to the variable z, i.e. $f'(z) = \partial f/\partial z$. Also, the displacement components are written in terms of the complex potentials Φ_1 and Φ_2 as:

$$\begin{aligned}
(w)_x &= 2\Re[p_1\Phi_1(z_1) + p_2\Phi_2(z_2)] - \omega y, \\
(w)_y &= 2\Re[q_1\Phi_1(z_1) + q_2\Phi_2(z_2)] + \omega x,
\end{aligned} \tag{B.4}$$

where ω characterize a rotation and the complex numbers p_i and q_i are:

$$
\begin{aligned}
p_i &= \alpha_{11}\mu_i^2 + \alpha_{12} - \alpha_{13}\mu_i, \\
q_i &= \alpha_{12}\mu_i + \alpha_{22}/\mu_i - \alpha_{23}, \quad i = 1, 2.
\end{aligned}
\tag{B.5}
$$

The complex potentials Φ_1 and Φ_2 are related to the stress function $F(x, y)$ by means of the relations:

$$
\Phi_1 = \frac{\partial F}{\partial z_1} \quad \text{and} \quad \Phi_2 = \frac{\partial F}{\partial z_2}.
\tag{B.6}
$$

In order to facilitate the notation, in the sequel we use the following definitions:

$$
\sigma_\varepsilon^e := \sigma_\varepsilon(w)|_{\Omega \setminus \overline{B_\varepsilon}} \quad \text{and} \quad \sigma_\varepsilon^i := \sigma_\varepsilon(w)|_{B_\varepsilon}.
\tag{B.7}
$$

Now, by applying the traction boundary condition on ∂B_ε, see (B.1)$_5$, and in view of the fact that the stress inside of the inclusion B_ε is constant, see [33,34], the complex potential for the solution outside B_ε, can be written as:

$$
\begin{aligned}
\Phi_1(z_1) &= \frac{1}{2(\mu_1 - \mu_2)} [((\sigma_\varepsilon^i)_{xx} + S_{xx})i - ((\sigma_\varepsilon^i)_{xy} + S_{xy})(1 - i\mu_2) - ((\sigma_\varepsilon^i)_{yy} + S_{yy})\mu_2]\frac{1}{\zeta_1} \\
\Phi_2(z_2) &= -\frac{1}{2(\mu_1 - \mu_2)} [((\sigma_\varepsilon^i)_{xx} + S_{xx})i - ((\sigma_\varepsilon^i)_{xy} + S_{xy})(1 - i\mu_1) - ((\sigma_\varepsilon^i)_{yy} + S_{yy})\mu_1]\frac{1}{\zeta_2}
\end{aligned}
\tag{B.8}
$$

where S_{ij} and $(\sigma_\varepsilon^i)_{ij}$ are the components of tensors S and σ_ε^i, respectively, measured in the coordinate system (x, y), and

$$
\zeta_k = \frac{z_k + \sqrt{z_k^2 - 1 - \mu_k^2}}{1 - i\mu_k} \quad \text{with} \quad k = 1, 2.
\tag{B.9}
$$

Note that expression (B.8) indicates that the stress field outside the inclusion B_ε can be explicitly obtained in terms of the boundary condition on ∂B_ε and the stress inside B_ε. The components of σ_ε^e can be obtained by inserting the potentials (B.8) in (B.3).

Next, by applying the displacement boundary condition (B.1)$_4$, see ([24], Chapter VI, Section 41), we obtain the following system of equations, which will define the four unknown: components of the stress σ_ε^i and the rotation of the inclusion ω,

$$
Ks = Fs_m,
\tag{B.10}
$$

where matrices K and F; and vectors s and s_m are given by:

$$
K = \begin{pmatrix}
-(\Im[\kappa] + \alpha_{11}^\star) & -(\Re[\lambda] + \alpha_{12}^\star) & -(\Re[\kappa] + \Im[\lambda] + \alpha_{13}^\star) & 0 \\
\Re[\kappa] & -\Im[\lambda] & \Re[\lambda] - \Im[\kappa] & 1 \\
-(\Im[\gamma] + \alpha_{13}^\star) & -(\Re[\rho] + \alpha_{23}^\star) & -(\Re[\gamma] + \Im[\rho] + \alpha_{33}^\star) & -1 \\
\Re[\gamma] - \alpha_{12}^\star & -(\Im[\rho] + \alpha_{22}^\star) & \Re[\rho] - \Im[\gamma] - \alpha_{32}^\star & 0
\end{pmatrix}
\tag{B.11}
$$

$$
s = \begin{pmatrix}
(\sigma_\varepsilon^i)_{xx} \\
(\sigma_\varepsilon^i)_{yy} \\
(\sigma_\varepsilon^i)_{xy} \\
\omega
\end{pmatrix}
\tag{B.12}
$$

$$
F = \begin{pmatrix}
\Im[\kappa] & \Re[\lambda] & \Im[\lambda] + \Re[\kappa] \\
-\Re[\kappa] & \Im[\lambda] & -\Re[\lambda] + \Im[\kappa] \\
\Im[\gamma] & \Re[\rho] & \Im[\rho] + \Re[\gamma] \\
-\Re[\gamma] & \Im[\rho] & -\Re[\rho] + \Im[\gamma]
\end{pmatrix}
\tag{B.13}
$$

$$
s_m = \begin{pmatrix}
S_{xx} \\
S_{yy} \\
S_{xy}
\end{pmatrix}.
\tag{B.14}
$$

In the above system of equations, $\Re[\bullet]$ and $\Im[\bullet]$ are used to denote the real and imaginary part of $[\bullet]$, respectively. Also, $\alpha_{ij}^{\star}$, with $(i, j) = 1..3$, are the components of $(\mathbb{C}^{\star})^{-1}$ (in matrix notation) and the complex number ρ, λ, γ and κ are given by:

$$\rho = \frac{q_1\mu_2 - q_2\mu_1}{\mu_1 - \mu_2}, \quad \gamma = \frac{q_1 - q_2}{\mu_1 - \mu_2}, \quad \kappa = \frac{p_1 - p_2}{\mu_1 - \mu_2} \quad \text{and} \quad \lambda = \frac{p_1\mu_2 - p_2\mu_1}{\mu_1 - \mu_2}. \tag{B.15}$$

Then, in view of the system (B.10) the stress inside of the inclusion can be obtained as:

$$\begin{pmatrix} (\sigma_\varepsilon^i)_{xx} \\ (\sigma_\varepsilon^i)_{yy} \\ (\sigma_\varepsilon^i)_{xy} \end{pmatrix} = A s_m \tag{B.16}$$

where matrix A is given by the first three rows of $K^{-1}F$. The components of matrix A are not explicitly given here due to their complexity.

Finally, by rearranging (B.16), the solution of (B.1) in B_ε can be written in tensorial notation as a function of the boundary condition in ∂B_ε:

$$\sigma_\varepsilon(w)|_{B_\varepsilon} = \mathbb{A}S, \tag{B.17}$$

where components of the tensor $\mathbb{A}$ are related to components of the matrix A by the standard contracted notation (or Voigt notation) using the following rules for replacing the subscript:

$$11 \to 1, \quad 22 \to 2 \quad \text{and} \quad 12 \to 3. \tag{B.18}$$

In view of the symmetries of $\sigma_\varepsilon(w)$ and S, the tensor $\mathbb{A}$ has the following symmetry properties:

$$\mathbb{A}_{ijkl} = \mathbb{A}_{jikl} \quad \text{and} \quad \mathbb{A}_{ijkl} = \mathbb{A}_{ijlk}. \tag{B.19}$$

References

[1] A.A. Novotny, J. Sokołowski, Topological derivatives in shape optimization, in: Interaction of Mechanics and Mathematics, Springer-Verlag, Berlin, Heidelberg, 2013.

[2] J. Sokołowski, A. Zochowski, On the topological derivative in shape optimization, SIAM J. Control Optim. 37 (4) (1999) 1251–1272.

[3] R. Amigo, S. Giusti, A. Novotny, E. Silva, J. Sokolowski, Optimum design of flextensional piezoelectric actuators into two spatial dimensions, SIAM J. Control Optim. 52 (2) (2016) 760–789.

[4] A.J. Torii, A.A. Novotny, R.B. Santos, Robust compliance topology optimization based on the topological derivative concept, Internat. J. Numer. Methods Engrg. 106 (11) (2016) 889–903.

[5] H. Isaraki, K. Kuriyama, S. Harada, T. Yamada, T. Takahashi, T. Matsumoto, A topology optimisation for three-dimensional acoustics with the level set method and the fast multipole boundary element method, Mech. Eng. J. 1 (4) (2014) 1–13.

[6] S. Amstutz, A.A. Novotny, E.A. de Souza Neto, Topological derivative-based topology optimization of structures subject to Drucker-Prager stress constraints, Comput. Methods Appl. Mech. Engrg. 233–236 (2012) 123–136.

[7] J.R. de Faria, D. Lesnic, Topological derivative for the inverse conductivity problem: A bayesian approach, J. Sci. Comput. 63 (1) (2015) 256–278.

[8] S.M. Giusti, A.A. Novotny, E.A. de Souza Neto, R.A. Feijóo, Sensitivity of the macroscopic elasticity tensor to topological microstructural changes, J. Mech. Phys. Solids 57 (3) (2009) 555–570.

[9] N. Van Goethem, A.A. Novotny, Crack nucleation sensitivity analysis, Math. Methods Appl. Sci. 33 (16) (2010) 197–1994.

[10] G. Allaire, F. de Gournay, F. Jouve, A.M. Toader, Structural optimization using topological and shape sensitivity via a level set method, Control Cybernet. 34 (1) (2005) 59–80.

[11] T. Yamada, K. Izui, S. Nishiwaki, A. Takezawa, A topology optimization method based on the level set method incorporating a fictitious interface energy, Comput. Methods Appl. Mech. Engrg. 199 (2010) 2876–2891.

[12] G. Cardone, S. Nazarov, J. Sokołowski, Asymptotic analysis, polarization matrices, and topological derivatives for piezoelectric materials with small voids, SIAM J. Control Optim. 48 (6) (2010) 3925–3961.

[13] J. Sokołowski, A. Zochowski, Optimality conditions for simultaneous topology and shape optimization, SIAM J. Control Optim. 42 (4) (2003) 1198–1221.

[14] G. Pólya, G. Szegö, Izoperimetric Inequalities in Mathematical Physics, Princeton University Press, Princeton, 1951.

[15] H. Ammari, H. Kang, Polarization and moment tensors with applications to inverse problems and effective medium theory, in: Applied Mathematical Sciences, vol. 162, Springer-Verlag, New York, 2007.

[16] S.M. Giusti, A.A. Novotny, Topological derivative for an anisotropic and heterogeneous heat diffusion problem, Mech. Res. Commun. 46 (2012) 26–33.

[17] S.M. Giusti, L.M.A. Mello, E.C.N. Silva, Piezoresistive device optimization using topological derivative concepts, Struct. Multidiscip. Optim. 50 (2014) 453–464.
[18] S.M. Giusti, A.A. Novotny, J. Sokołowski, Topological derivative for steady-state orthotropic heat diffusion problem, Struct. Multidiscip. Optim. 40 (1) (2010) 53–64.
[19] E. Beretta, E. Bonnetier, E. Francini, A.L. Mazzucato, Small volume asymptotics for anisotropic elastic inclusions, Inverse Probl. Imaging 6 (1) (2012) 1–23.
[20] S.A. Nazarov, J. Sokołowski, M. Specovius-Neugebauer, Polarization matrices in anisotropic heterogeneous elasticity, Asymptot. Anal. 68 (4) (2010) 189–221.
[21] M. Bonnet, G. Delgado, The topological derivative in anisotropic elasticity, Quart. J. Mech. Appl. Math. 66 (4) (2013) 557–586.
[22] V.A. Kozlov, V.G. Maz'ya, A.B. Movchan, Asymptotic Analysis of Fields in Multi-structures, Clarendon Press, Oxford, 1999.
[23] S.G. Lekhnitskii, Theory of elasticity of an anisotropic elastic body, in: Holden-Day Series in Mathematical Physics, Holden-Day, Inc., San Francisco, California, 1963.
[24] S.G. Lekhnitskii, S.W. Tsai, T. Cheron, Anisotropic Plates, Gordon and Breach Science Publishers, New York, U.S.A, 1968.
[25] S. Amstutz, H. Andrä, A new algorithm for topology optimization using a level-set method, J. Comput. Phys. 216 (2) (2006) 573–588.
[26] S. Osher, J.A. Sethian, Front propagating with curvature dependent speed: algorithms based on Hamilton–Jacobi formulations, J. Comput. Phys. 79 (1) (1988) 12–49.
[27] S. Amstutz, S.M. Giusti, A.A. Novotny, E.A. de Souza Neto, Topological derivative for multi-scale linear elasticity models applied to the synthesis of microstructures, Internat. J. Numer. Methods Engrg. 84 (2010) 733–756.
[28] S. Amstutz, A.A. Novotny, Topological optimization of structures subject to von Mises stress constraints, Struct. Multidiscip. Optim. 41 (3) (2010) 407–420.
[29] D.E. Campeão, S.M. Giusti, A.A. Novotny, Topology design of plates consedering different volume control methods, Eng. Comput. 31 (5) (2014) 826–842.
[30] C.G. Lopes, R.B. dos Santos, A.A. Novotny, Topological derivative-based topology optimization of structures subject to multiple load-cases, Lat. Am. J. Solids Struct. 12 (2015) 834–860.
[31] S. Amstutz, Analysis of a level set method for topology optimization, Optim. Methods Softw. 26 (4–5) (2011) 555–573.
[32] E. Sanchez-Palencia, Non-homogeneous media and vibration theory, in: Lecture Notes in Physics, vol. 127, Springer-Verlag, Berlin, 1980.
[33] J.D. Eshelby, The determination of the elastic field of an ellipsoidal inclusion, and related problems, Proc. R. Soc.: A 241 (1957) 376–396.
[34] J.D. Eshelby, The elastic field outside an ellipsoidal inclusion, and related problems, Proc. R. Soc. A 252 (1959) 561–569.